Evaluation of Normal Human Foveal Development Using Optical Coherence Tomography and Histologic Examination

Adam M. Dubis, PhD; Deborah M. Costakos, MD, MSc; C. Devika Subramaniam, MD; Pooja Godara, MD; William J. Wirostko, MD; Joseph Carroll, PhD; Jan M. Provis, PhD

Objective: To assess outer retinal layer maturation during late gestation and early postnatal life using optical coherence tomography and histologic examination.

Methods: Thirty-nine participants 30 weeks' postmenstrual age or older were imaged using a handheld optical coherence tomography system, for a total of 102 imaging sessions. Foveal images from 16 participants (21 imaging sessions) were normal and evaluated for inner retinal excavation and the presence of outer retinal reflective bands. Reflectivity profiles of central, parafoveal, and parafoveal retina were extracted and were compared with age-matched histologic sections.

Results: The foveal pit morphologic structure in infants was generally distinguishable from that in adults. Reflectivity profiles showed a single hyperreflective band at the fovea in all the infants younger than 42 weeks' postmenstrual age. Multiple bands were distinguishable in the outer retina at the peri fovea by 32 weeks' postmenstrual age and at the fovea by 3 months' postterm. By 17 months' postnatal, the characteristic appearance of 4 hyperreflective bands was evident across the foveal region. These features are consistent with previous results from histologic examinations. A "temporal divot" was present in some infants, and the foveal pit morphologic structure and the extent of inner retinal excavation were variable.

Conclusions: Handheld optical coherence tomography is a viable technique for evaluating neonatal retinas. In premature infants who do not develop retinopathy of prematurity, the foveal region seems to follow a developmental time course similar to that associated with in utero maturation.

Clinical Relevance: As pediatric optical coherence tomography becomes more common, a better understanding of normal foveal and macular development is needed. Longitudinal imaging offers the opportunity to track postnatal foveal development among preterm infants in whom poor visual outcomes are anticipated or to follow up treatment outcomes in this population.

Arch Ophthalmol. 2012;130(10):1291-1300

Author Affiliations:
Departments of Cell Biology, Neurobiology, and Anatomy (Drs Dubis and Carroll), Ophthalmology (Drs Costakos, Subramaniam, Godara, Wirostko, and Carroll), and Biophysics (Dr Carroll), Medical College of Wisconsin, and Children's Hospital of Wisconsin (Dr Costakos), Milwaukee; and Australian Research Council Centre of Excellence in Vision Science, The John Curtin School of Medical Research and Australian National University Medical School, Australian National University, Canberra (Dr Provis). Dr Dubis is now with Duke Eye Center, Durham, North Carolina.

THE FOVEA CENTRALIS IS A feature of all anthropoid primate retinas. The foveal avascular zone (FAZ), increased cone density, and excavation of inner retinal neurons characterize the foveal region. The most salient feature of the human fovea is the shallow pit that is left behind by the lateral displacement of the inner retinal layers (*fovea* is Latin for pit). Before and during foveal formation, cones become tightly packed, elongate, and migrate centripetally.[1-3] The processes of cone packing and pit development in humans have been examined in histologic studies.[1-7] Whereas the site of the future fovea can be identified as early as 12 weeks' postmenstrual age (PMA) using morphologic criteria[3,8] and molecular cues,[7,9-12] the pit itself does not emerge until after the FAZ is defined at around 24 to 26 weeks' PMA. Subsequent gestational changes include centrifugal migration of inner retinal neurons, resulting in progressive reduction of

the ganglion and bipolar cell layers at the fovea. During the last trimester, photoreceptors are immature at the foveal center compared with those at parafoveal and parafoveal locations.[13] During this period, the retinal pigment epithelium (RPE) also develops interdigitations with the immature outer segments.[1,2,7] Postnatally, the foveal pit contour continues to be modified by cellular migration, reaching maturity at roughly 18 months' postterm.[2] Photoreceptor elongation and displacement into the fovea also continue postna-

tally, and the results of studies[1,2] indicate that foveal cone density reaches the lower range reported for adults by age 4 years. The exact relationship between the foveal pit development and the photoreceptor mosaic maturation remains unclear.[3,14,15]

Optical coherence tomography (OCT) enables visualization of the retinal lamina and the organization of the outer retina.[16-18] Previously, the use of OCT had been limited to cooperative and fixating individuals. However, the recent availability of handheld systems enables imaging of pediatric populations, with clinical applications that include pediatric abusive head trauma[19,20] and retinopathy of prematurity (ROP).[21-23] Recent work from one group has aimed to increase the efficiency of pediatric OCT, providing some insights into normal development.[24,25] Advances in OCT image acquisition,[26,27] with reinvestigation by anatomists,[17,28] have raised questions about the initial anatomical assignment of layers observed with OCT.[16,18,25,26] Defining the correlation between OCT bands and photoreceptor structure is important for understanding foveal development.

Using handheld OCT, we examined postnatal features of foveal development in a series of pediatric patients.[1,2,7,8,23,25] Across individuals of different ages, we compared emerging retinal layers in OCT with those in age-matched histologic sections. We used these comparisons and information available in the literature[17,18] to define reflectance bands in pediatric OCT images. We also examined the variability in the foveal pit morphologic structure among this pediatric population. A better understanding of what is visualized by OCT will enable reliable interpretation of in vivo developmental data and will facilitate the identification of normal vs pathologic features in a clinical setting.

METHODS

PARTICIPANTS

Research on humans followed the tenets of the Declaration of Helsinki and was approved by institutional review boards at the Medical College of Wisconsin and at Children's Hospital of Wisconsin. Informed consent was obtained from parents of all the minors after explanation of the nature and possible consequences of the study. One adult participant provided his own consent. Thirty-nine participants (26 male and 13 female) 30 weeks' PMA or older were recruited from local communities surrounding the Medical College of Wisconsin. Thirty-five participants were recruited from the neonatal intensive care unit at Children's Hospital of Wisconsin for an examination using anesthesia, as well as 4 participants at the Medical College of Wisconsin Eye Institute. For imaging, eyes were dilated and accommodation suspended using a combination cyclopentolate hydrochloride–phenylephrine hydrochloride ophthalmic solution. Artificial tears were used in all the participants (saline drops or a combination of polyethylene glycol–propylene glycol). For the infants, a eyelid speculum was used during imaging to keep the eye open. Imaging was performed after clinical evaluation in all the cases. To be considered healthy for this study, at no time could participants have developed cystoid macular edema (CME) or have had ROP worse than stage 2, consistent with previously used criteria.[25] One of us (D.M.C.) assessed the progression of ROP, and the presence of CME on OCT images was determined by consensus of 4 graders (A.M.D., D.M.C., C.D.S., and P.G.).

HANDHELD PROBE SPECTRAL-DOMAIN OCT

Optical coherence tomography was performed using a handheld probe spectral-domain OCT system (HHP-SDOCT; Bioptigen). Reference arm position and instrument focus were initially set on the basis of information provided by Maldonado et al,[24] with additional adjustments performed if required to improve image quality. The nominal image size for all the participants was 8×8 mm, with an image density of 1000 A-scans per 100 B-scans (except for participant DC_0368, for whom the nominal image size was a 6×6-mm cube). The setting assumes an axial length of 24 mm; however, given the shorter axial length of our population, the actual image length is less (approximately 6 mm). Individual variation in axial length would further alter the image length for each participant. This provides a slightly different lateral resolution for each individual; however, this image size was selected to cover the maximum amount of retinal area (allowing visualization of the macula and the edge of the optic nerve in a single image). Images were exported in an audiovisual interleaving format using on-instrument software (Bioptigen In Vivo Vue Clinic; Bioptigen), and frames containing photographs of the macula were extracted.

HISTOLOGIC EXAMINATION

Histologic images were selected from a database assembled from human and macaque retinal histologic sections collected by one of us (J.M.P.) and by Anita Hendrickson, PhD, at the Department of Biological Structure, University of Washington, Seattle. Montages were assembled from high-resolution images obtained using a digital camera (HP; Carl Zeiss) through an 25× objective lens (Carl Zeiss), at a final optical magnification of 312.5×, between January 1, 1995, and January 27, 2012, at the University of Washington or at the Australian National University, Canberra. Sections were montages created by one of us (J.M.P.) using available software (Photoshop CS5; Adobe Systems Incorporated). Macaque tissue was paraffin embedded, while all the human samples were embedded in methacrylate; both sample types were stained with Richardson stain.

AGE-MATCHED AND LAYER-MATCHED HISTOLOGIC SECTIONS AND OCT IMAGES

Optical coherence tomography images were age matched with 3 histologic images of human retinas at 35 weeks' PMA, 41 weeks' PMA, and 13 years' postterm. Because of the rarity of human donor retinas between 25 and 40 weeks' PMA, we selected images from macaque retinas at fetal day 131 as approximately equivalent to the human retina at 32 weeks' PMA. To establish a valid comparative time point, we used the cecal period (CP) (the period between conception and eye opening) as a unit of development. The CP is 196 days (28 weeks) long in humans compared with 123 days (almost 18 weeks) in macaques. Initial formation of the fovea is dependent on the definition of the FAZ, which occurs at around 85% CP in macaques but occurs slightly later in humans at approximately 90% CP (**Table**). Thirty-two weeks' PMA (224 days postconception) in humans is 44 days after the definition of the FAZ, which is equivalent to 22% CP in humans. Twenty-two percent CP in macaques is 27 days; 27 days after the definition of the macaque FAZ is 133 days postconception. The fetal day 131 retina is the closest approximation to 32 weeks' PMA among the humans available in our data set. Optical coherence tomography data from an infant of 35 weeks' PMA were compared with histologic sample data from a human donor of 35 weeks' PMA. Optical coherence tomography data from an infant of 40 weeks'

Table. Initial Formation of the Fovea Is Dependent on the Definition of the Foveal Avascular Zone (FAZ)

Fovea	Eye Opening	Birth	Approximate Definition of the FAZ	Comparative Time Point
Human	196 d Postconception (100% CP) [28 wk PMA]	280 d Postconception (143% CP) [40 wk PMA]	180 d Postconception (90% CP) [25-26 wk PMA]	224 d Postconception (22% CP) [44 d after definition of the FAZ]
Macaque	123 d Postconception (100% CP)	172 d Postconception (138% CP)	100-105 d Postconception (85% CP)	133 d Postconception (22% CP) [27 d after definition of the FAZ]

Abbreviations: CP, cecal period; PMA, postmenstrual age.

PMA were compared with histologic sample data from a human donor of 41 weeks' PMA. Finally, OCT data from an adult aged 28 years and from a child aged 17 months were compared with histologic sample data from a human aged 13 years.

For comparisons of OCT images and histologic section data, we assigned 5 bands (numbered from 0 to 4) to the outer retinal layers. Bands 1 through 4 were assigned based on recent work by Spaide and Curcio,[28] with an additional band 0 at the interface between the outer plexiform layer and the outer nuclear layer, which includes the photoreceptor pedicles and synapses. Band 1 was assigned to the external limiting membrane (ELM). Band 2 was assigned to the inner segment ellipsoid.[29] Bands 3 and 4 are composed of the photoreceptor and RPE microvilli interface and the RPE and Bruch membrane, respectively.

QUALITATIVE ANALYSIS

The lateral scales for OCT image data and histologic sample data were adjusted to facilitate comparisons at specific locations. Histologic images were calibrated from the original corresponding grid images, while OCT images were corrected based on age-specific axial length estimates previously reported.[24] Longitudinal reflectivity profiles (LRPs) were generated from OCT images using available software (ImageJ; National Institutes of Health).[30] To increase the ratios of signal to noise and to facilitate band assignment, gray-scale reflectivity values from 5 consecutive lateral positions were averaged to construct each LRP. The LRPs were analyzed for the presence or absence of each of 5 outer retinal bands in the fovea (central 0.5 mm, approximately 1.5° visual angle), parafovea (0.5-mm to 1.0-mm eccentricity, approximately 3° nasal), and perifovea (2-mm eccentricity, approximately 6° nasal). The congruency in band assignment across OCT images, LRPs, and histologic sections is shown in **Figure 1**.

RESULTS

PARTICIPANTS IMAGED

As summarized in the eTable (available at: http://www.archophthalmol.com), we obtained clinically usable images in 72.4% (71 of 98) of examinations among awake infants in the neonatal intensive care unit and in 100.0% (4 of 4) imaged as part of an examination using anesthesia. We defined *clinically usable* as a volume image in which the foveal center and both slopes were visible with sufficient image quality for the graders to determine the presence or absence of CME. These results are comparable to those in other studies.[22,25] The 75 clinically usable images were acquired from 33 participants. Because the present study was designed to assess normal foveal development, participants whose findings were deemed abnormal (those with development of CME, occurrence of greater than stage
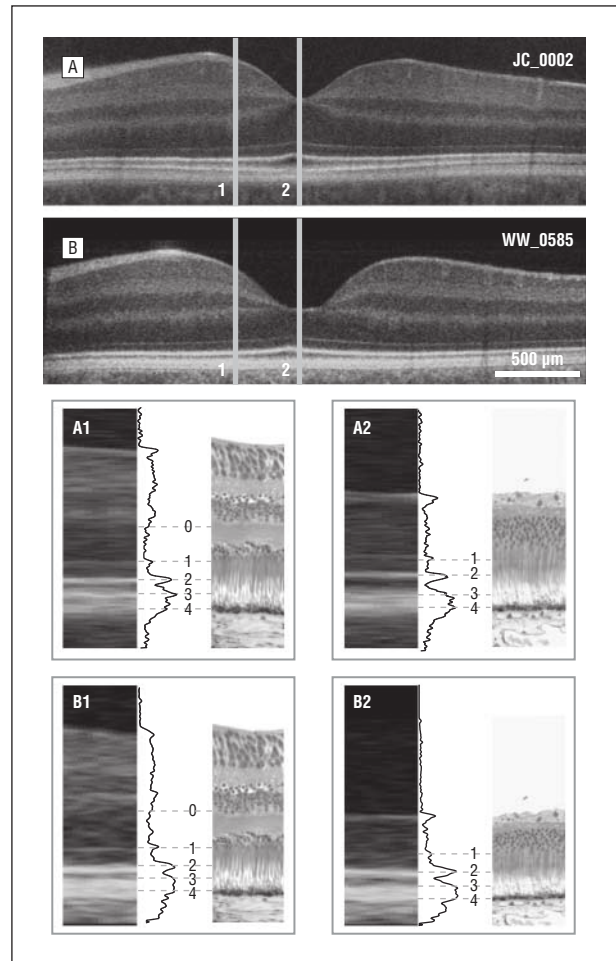

Figure 1. Foveal layer assignment in the human retina. A, Shown is an optical coherence tomography image of a 28-year-old retina (JC_0002). B, A 17-month-old retina (WW_0585) is compared with histologic images at parafoveal (1) and foveal (2) locations. A1 and B1 show the assignment of outer retinal layer bands 0 through 4, illustrated with gray lines connecting the optical coherence tomography image, longitudinal reflectivity profile, and histologic image for the parafoveal area. Band assignments in the foveal region are shown in A2 and B2.

2 ROP, or requirement of an intervention for ROP) were excluded from subsequent analysis. Five of 33 participants were excluded because they developed stage 3 ROP or required an intervention for ROP, while 12 were excluded because they developed CME. Foveal images from the remaining 16 participants (15 male and 1 female) were considered normal for this study. The 21 images from these individuals are shown in **Figure 2**, with multiple images obtained from 3 participants (2 images from DC_0499 and 3 images each from DC_0576 and DC_0688).
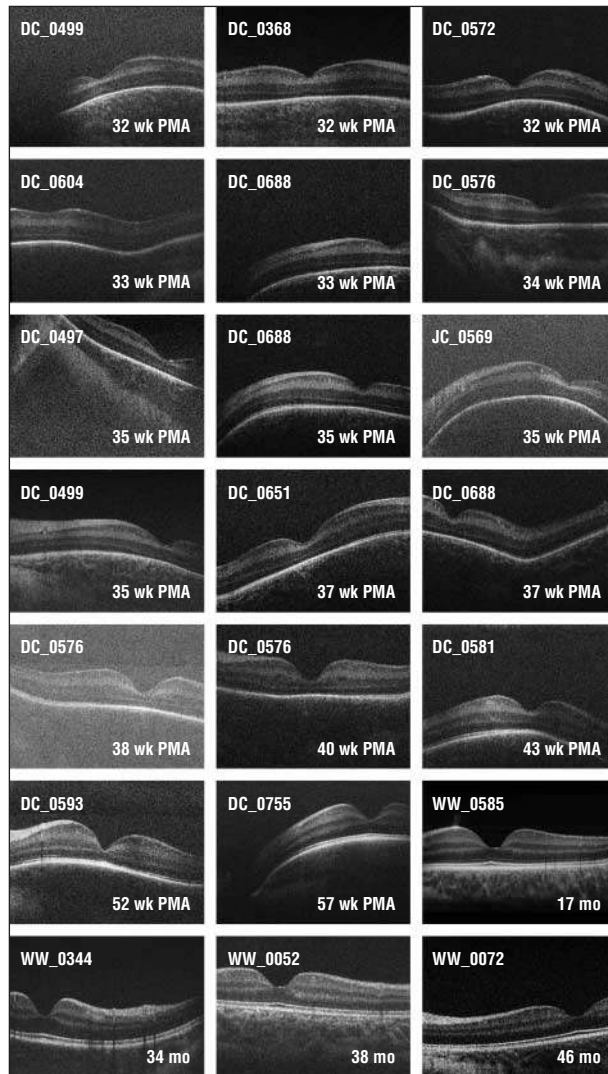
Figure 2. Spectrum of the foveal pit morphologic structure observed with optical coherence tomography. Shown are foveal images from all examinations meeting the inclusion criteria. Images are single frames extracted from a macular volume. Considerable variability exists at the stage of 32 weeks' to 33 weeks' postmenstrual age (PMA). By age 17 months, the retina appears adultlike. Another notable feature is that some individuals have a diplike structure located temporal to the macula (DC_0604 at 33 weeks' PMA, DC_0576 at 34 weeks' PMA, and DC_0688 at 37 weeks' PMA). We refer to this structure as a "temporal divot."

PHOTORECEPTOR AND FOVEAL PIT MATURATION

As expected from histologic data, the foveal pit was present in images obtained from the youngest participant, an infant of 32 weeks' PMA.[2,25] Across the series of participants imaged, we observed variability in the foveal pit morphologic structure even among age-matched individuals (Figure 2). For example, the foveae of the 3 youngest participants (32 weeks' PMA) differ in appearance (Figure 2, top row); participant DC_0572 has a deeper depression than the other infants of 32 weeks' PMA, as well as the infants of 33 weeks' PMA in the second row. In this series, the foveal pit continues to deepen and widen through 43 weeks' PMA but is still immature at this point, having a distinct inner nuclear layer lining the floor of the pit. The participant of 52 weeks' PMA (DC_0593) is the youngest to show complete excavation of all inner retinal layers.

In all the participants younger than 43 weeks' PMA, only 2 hyperreflective bands were detected in the fovea. However, multiple hyperreflective bands were detected in the perifoveal region in even the youngest participants. In contrast to previous data,[25] we found the outer retina to be adultlike at 17 months' postnatal in terms of the characteristic appearance of 4 hyperreflective bands.

MACAQUE FETAL DAY 131 TO HUMAN 32 WEEKS' PMA

In an OCT image at 32 weeks' PMA (**Figure 3**), a distinct band, which we refer to as band 0, crosses the fovea. After examining a range of specimens, we conclude that band 0 reflects the layer of cone pedicles. A thicker hyperreflective band is present at the level of the RPE and the RPE $\times$ photoreceptor interaction, which we refer to as band 3/4. This is consistent with the appearance of the histologic image, which shows that the foveal photoreceptor nuclei are only a single layer deep but have short axons that separate the cone pedicles from the layer of nuclei. The foveal photoreceptors have short inner and outer segments that are barely distinguishable from the RPE. In the parafovea, the OCT image shows an increase in the separation between these 2 hyperreflective bands, indicative of increased elongation of photoreceptor cells in the parafovea compared with the fovea. This is consistent with the features seen in the macaque fetal day 131 histologic section, which shows that parafoveal cones have smaller soma diameters and longer axons compared with foveal cones (Figure 3C1 and C2). This difference would account for the increased separation between the hyperreflective bands in the parafovea. In the perifovea, a broadening of the outermost band is observed in the OCT image, seen as a double peak in the LRP profile (Figure 3C1). Comparison with the histologic image at this location indicates that, in addition to being more elongated than at the fovea, the photoreceptors in the perifovea have better developed inner and outer segments. Elongation of the outer segments results in the increased separation of the ELM from the RPE and accounts for the appearance of an additional band (band 1/2) in the perifoveal OCT image.

A feature of the OCT images from DC_0368 and DC_0499 but not DC_0572 (all 32 weeks' PMA) is the presence of an upward inflection in band 0 in the fovea. Such differences show that the enormous variability in foveal anatomy seen in adults likely has its origins early in development.

COMPARISON OF HUMAN HISTOLOGIC SECTIONS AND OCT IMAGES AT 35 WEEKS' PMA

An OCT image at 35 weeks' PMA (**Figure 4**B) shows increased excavation of the central fovea, which still includes all the retinal layers. This interpretation is consistent with the features of the histologic section from a
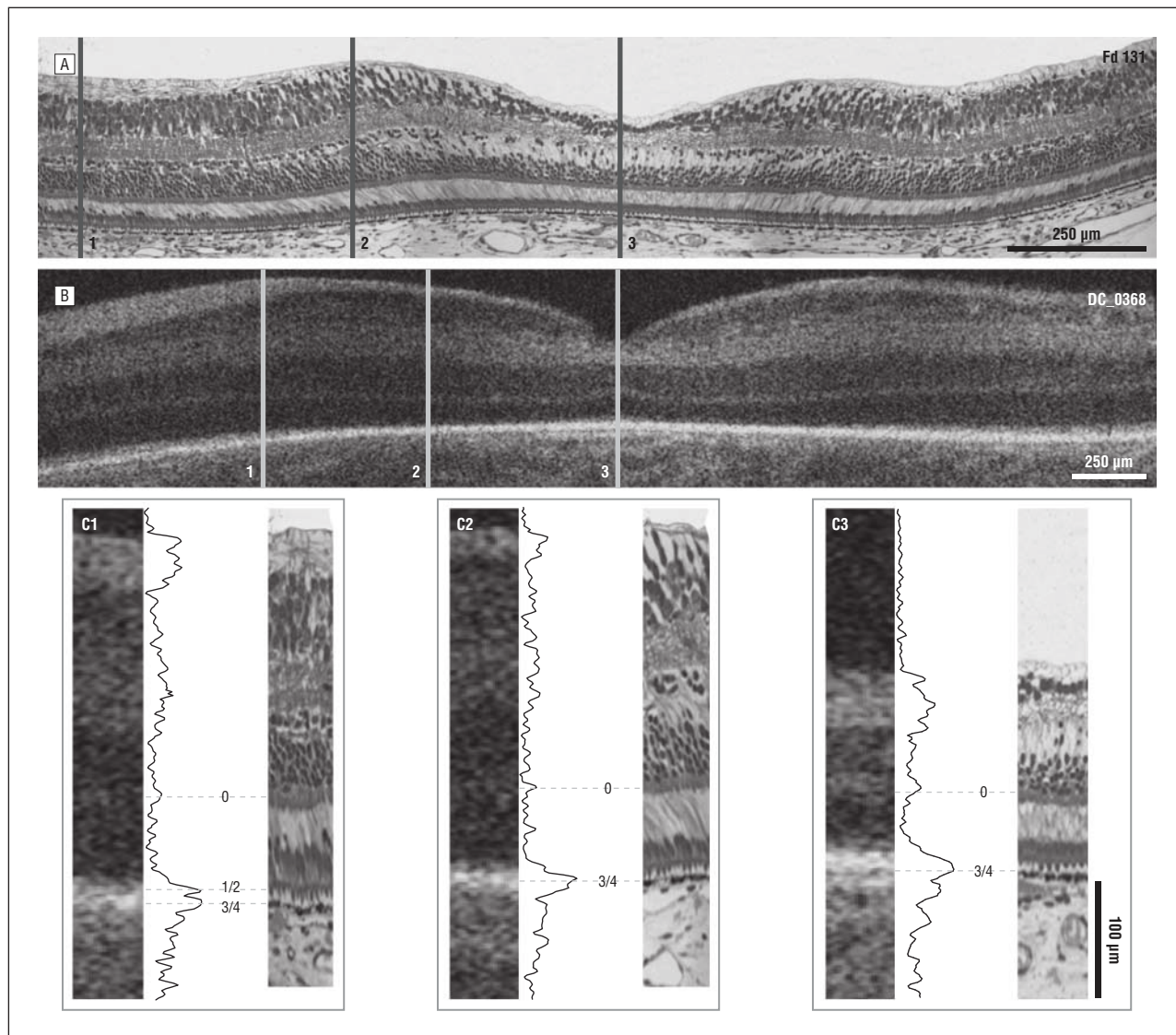
Figure 3. Comparison of foveal development and layer assignment in a macaque at fetal day (Fd) 131 (A) and in a human of 32 weeks' postmenstrual age (DC_0368) (B). Gray lines 1 through 3 represent perifoveal, parafoveal, and foveal locations, respectively. Insets C1 through C3 at the bottom are comparisons of histologic and optical coherence tomography images, with layer assignment for perifoveal (C1), parafoveal (C2), and foveal (C3) locations. At the perifoveal location, bands 0, 1/2, and 3/4 are present, whereas only bands 0 and 3/4 are present at the parafoveal and foveal locations.

human donor of 35 weeks' PMA (Figure 4A). The OCT image shows only 2 hyperreflective bands in the fovea (bands 0 and 3/4), consistent with histologic images showing foveal photoreceptors lacking well-formed outer segments that result in opposition of the ELM to the RPE (Figure 4C3). Although the histologic image shows that photoreceptors in the parafovea have somewhat more elongated cell bodies and rudimentary inner and outer segments, little increase is seen in the distance between the ELM and the RPE, consistent with the parafoveal OCT image showing only 2 hyperreflective bands (Figure 4C2). However, the perifoveal OCT image shows an additional band in the nasal outer retina (Figure 4C1). At a comparable location in the histologic section, photoreceptor inner and outer segments are more elongated than at the fovea (Figure 4C3), resulting in the better separation of the ELM from the RPE. This is consistent with the presence of an additional hyperreflective band in the OCT image, just emerging in the LRP, which most likely

corresponds to band 1/2.[28] Closer to the disc, the separation of band 1/2 from band 3/4 is more distinct. This is consistent with more advanced development of photoreceptors close to the disc at this age.

COMPARISON OF HUMAN HISTOLOGIC SECTIONS AND OCT IMAGES AT 41 WEEKS' PMA

Both OCT images and histologic sections at 41 weeks' PMA show foveae in all the retinal layers (**Figure 5**A and B). Although the histologic section demonstrates a broader, flatter fovea than the OCT image (probably owing to individual variation), both show a layer of cone pedicles (band 0 on the OCT image) at approximately 50% depth of the fovea (Figure 5C3). In the parafovea, the histologic section shows that the cell bodies of photoreceptors are more tightly packed than in the fovea; distinct inner segments and rudimentary outer segments are
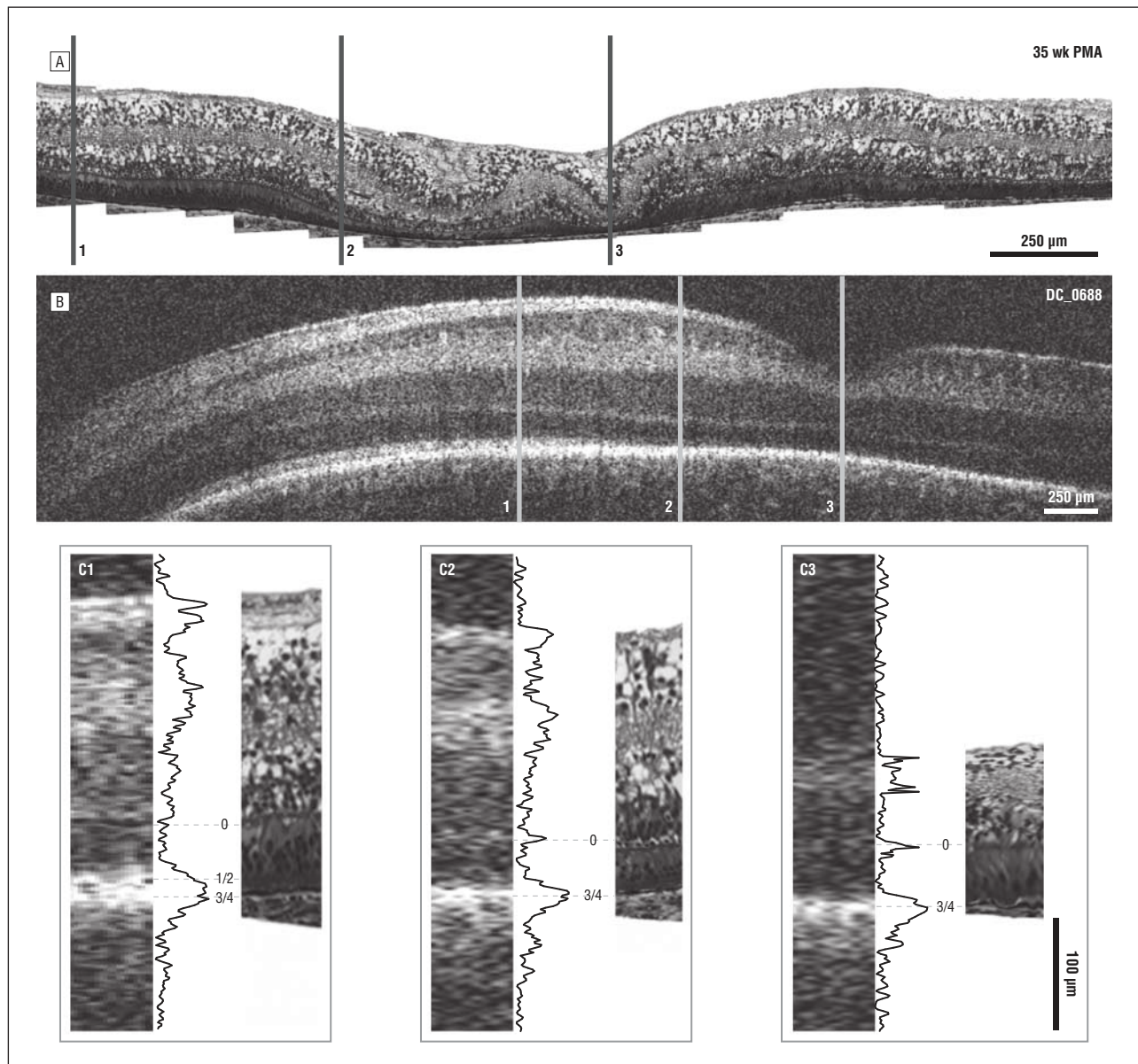
Figure 4. Comparison of foveal development and layer assignment. A, Histologic section from a human donor of 35 weeks' postmenstrual age (PMA). B, Infant of 35 weeks' PMA (DC_0688) imaged with optical coherence tomography (B). Gray lines 1 through 3 represent perifoveal, parafoveal, and foveal locations, respectively. Insets C1 through C3 at the bottom are comparisons of histologic and optical coherence tomography images, with layer assignment for perifoveal (C1), parafoveal (C2), and foveal (C3) locations. At the perifoveal location, bands 0, 1/2, and 3/4 are present, whereas only bands 0 and 3/4 are present at the parafoveal and foveal locations. The retina at 35 weeks' PMA shows moderate edema in the central fovea, which causes buckling of the retina (between C2 and C3) and blisterlike distortion of the innermost layer.

present such that the ELM and the RPE are separated by only a few microns (Figure 5C2). The OCT image at the parafovea is similar to that at the fovea, with only 2 hyperreflective bands present (bands 0 and 3/4). However, in the perifovea, the photoreceptor inner segments are more prominent than those in the fovea or parafovea, and the outer segments are better developed; these 2 changes result in a separation of the ELM and the RPE of approximately 42 μm at this location (Figure 5C1). Consistent with this advancing maturation, the OCT shows 4 distinct bands in the perifovea, which seem to correspond to the cone pedicles (band 0), ELM (band 1), inner segment ellipsoid (band 2), and RPE and outer segment associations (band 3/4).

The maturation sequence of foveal, parafoveal (1-mm eccentricity), and perifoveal (2-mm eccentricity) photoreceptors is shown in **Figure 6**, to which notional hyperreflectivity bands have been assigned. The sequence shows that the layer of cone pedicles is distinct at each location from about 30 weeks' PMA onward, and its position in the retinal profile makes this the most likely source of hyperreflective band 0. The foveal sequence (top row) suggests that the ELM begins to distinctly separate from the RPE only in the postnatal period and that the separation of bands 1 through 4 is unlikely to be observed until maturation of the foveal cones is almost complete. In developing retinas, the separation of the features associated with the hyperre-
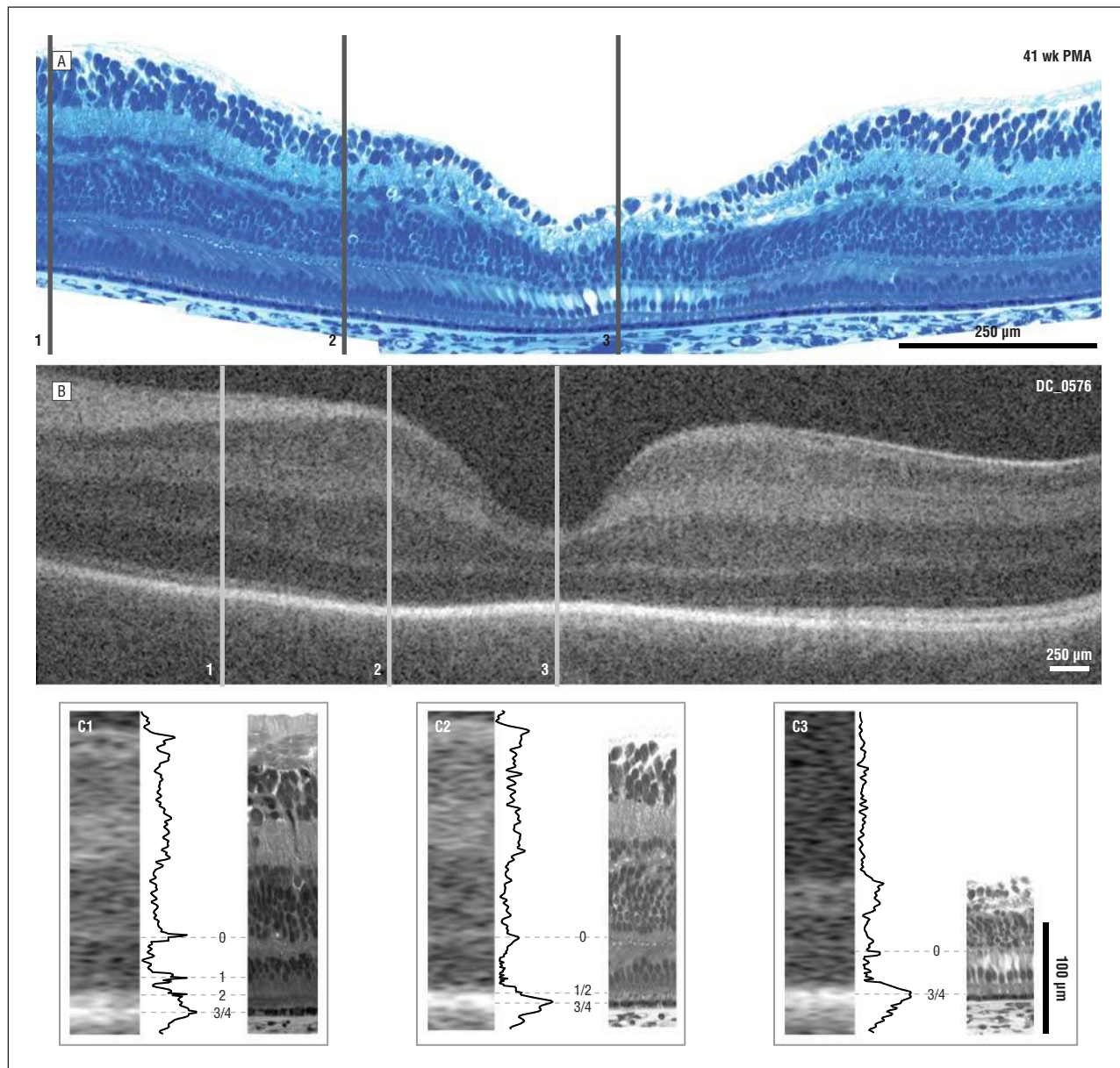
Figure 5. Comparison of foveal development and layer assignment in a histologic section from a human donor of 41 weeks' postmenstrual age (PMA) (A) and in an infant of 38 weeks' PMA (DC_0576) (B). Gray lines 1 through 3 represent perifoveal, parafoveal, and foveal locations, respectively. Insets C1 through C3 at the bottom are comparisons of histologic and optical coherence tomography images, with layer assignment for perifoveal (C1), parafoveal (C2), and foveal (C3) locations. At the perifoveal location, bands 0, 1, 2, and 3/4 are present, whereas only bands 0, 1/2, and 3/4 are present at the parafoveal location and bands 0 and 3/4 at the foveal location.

flective bands is better in the perifovea than in the parafovea, and both are better than that in the fovea. In the adult retina, the separation of bands 1 through 4 is most distinct in the fovea.

COMMENT

Foveal maturation and photoreceptor elongation can be studied in vivo using spectral-domain OCT among young infants, including those of premature age. Our imaging success rate of 72.4% in the neonatal intensive care unit is comparable to previous findings for similar populations[25] but is lower than that found by Vinekar et al,[22,31] who reported 100% success in 79 eyes using a different imaging system. Although the effects of CME and retinoschisis were not directly addressed in our study, they were present in 38.9% of the population, which differs from earlier data.[22,24] Uncooperative neonates and the use of an unsupported imaging arm provided challenges not encountered in adult imaging. Our methods differed somewhat from those by Maldonado et al,[24,25] we used an eyelid speculum and scleral depressor and chose to use a standard image size and off-line lateral correction based on age rather than change the image size.

This study provides further in vivo evidence that foveal development proceeds ex utero, consistent with other findings.[24] In addition, we observed variation in the foveal pit morphologic structure among age-
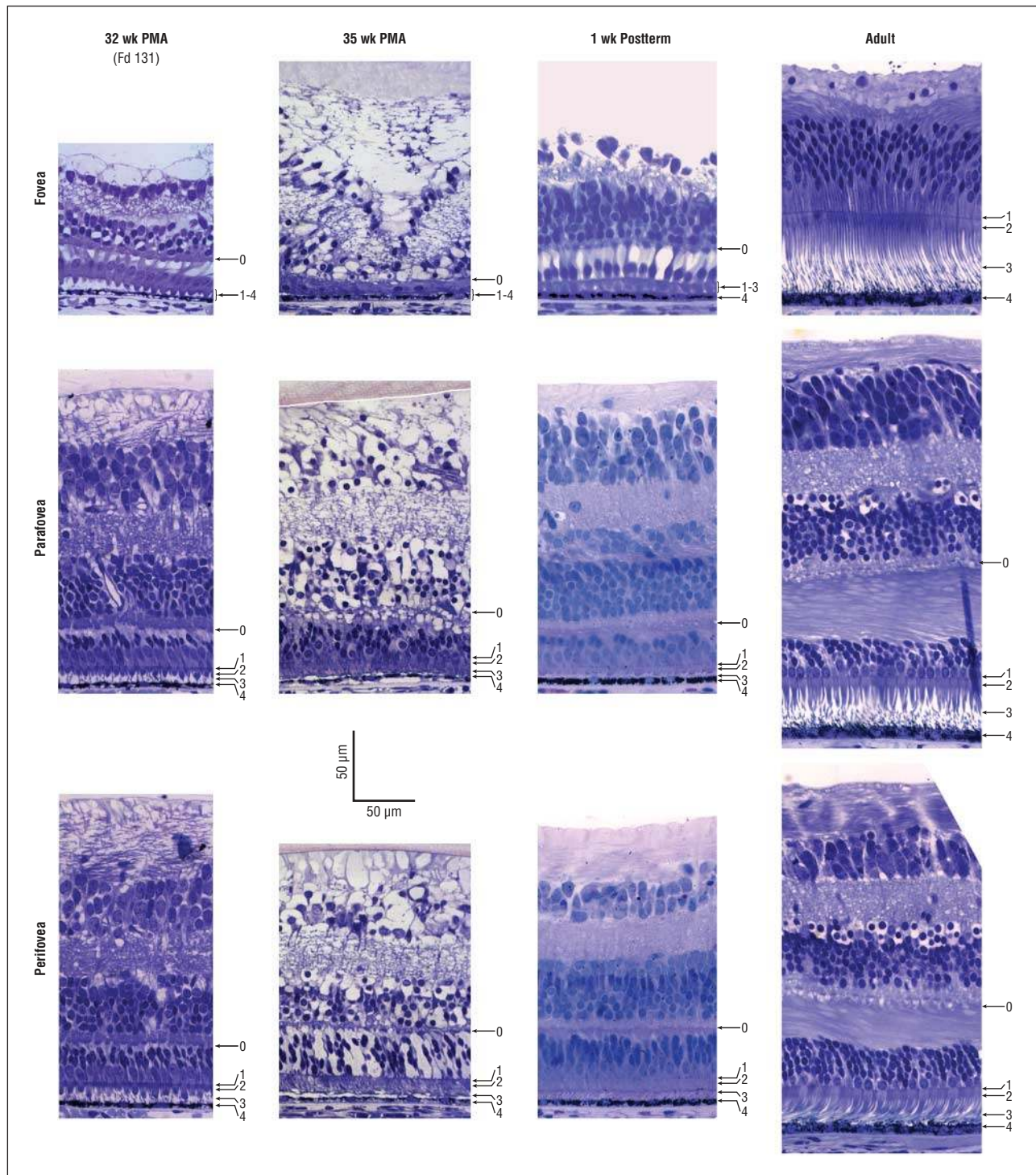
Figure 6. Time course of photoreceptor maturation at foveal (top row), parafoveal (middle row), and perifoveal (bottom row) locations. Images are labeled with band assignments as seen on optical coherence tomography. The retina at 35 weeks' postmenstrual age (PMA) shows moderate edema in the central fovea, which causes buckling of the retina and blisterlike distortion of the innermost layer; however, these tissue artifacts do not interfere with layer identification. Arrows indicate the presence of a distinct band (not layer thickness). Band 0 corresponds to the outer plexiform layer; band 1, the external limiting membrane; band 2, the inner segment ellipsoid; band 3, the retinal pigment epithelium × photoreceptor interdigitations; and band 4, the retinal pigment epithelium. Fd 131 indicates fetal day 131 in a macaque.

matched individuals in our study population. Two examples of this variability are seen in the infants of 32 weeks' and 33 weeks' PMA. In the 3 samples from infants of 32 weeks' PMA, variability is seen in photoreceptor layer thickness (distance from peak 0 to peak 3/4, which comprises the outer nuclear layer and the photo-

receptor inner segment and outer segment, if present). In 2 participants, the photoreceptor layer thickness decreases closer to the fovea, consistent with histologic data.[9,13,14] However in 2 participants at this age, a prominent upward tilt in band 0 is observed at the fovea, suggesting elongation of the central-most cones. Another

difference was that the infants of 33 weeks' PMA had shallower foveal depressions than the infants of 32 weeks' PMA. Participant DC_0604 had a residual ganglion cell layer at the fovea, while the other participants of 32 weeks' and 33 weeks' PMA did not. These developmental differences indicate that the enormous variability seen in adults originates during the earliest stages of foveal development.[32,33]

We also observed irregularities in the curvature of the retina in our study sample. Several eyes (ie, DC_0572, DC_0604, and DC_0688 in Figure 2) showed a sharp bend and an abrupt upward inflexion of the retina temporal to the parafovea in participants between 30 weeks' and 40 weeks' PMA; we refer to this as a "temporal divot." The bend appears to be at the temporal edge of the dome in the ganglion cell layer, formed by migrations of these cells[8]; the upward inflexion of the retina may reflect the contour of the sclera of a small eye. Irregularities in the contour of the developing eye are common in histologic preparations, commonly attributed to artifact due to retinal shrinkage and mechanical distortion. However, the presence of irregularities in vivo suggests a physiological explanation; one possibility is that retinal growth is not perfectly matched to scleral growth developmentally. The relationship of the retina to the sclera during the late stages of development could be addressed through longitudinal OCT studies.

Previous histologic findings suggest that the fovea continues to mature for several years after birth.[2] Our data indicate that morphologic development of the fovea may be complete by around 17 months, at least in some individuals. Maldonado et al[25] suggested that the retina is not fully mature at 15 months, citing an individual who lacked the separation of band 3/4, although the image was not shown. It is possible in the 2-month window from 15 months to 17 months that the photoreceptors undergo rapid elongation, rendering band 3 (RPE × photoreceptor interaction) separate from band 4. Alternatively, better image quality may reveal the separation of band 3 and band 4 in our neonates. Nevertheless, our findings and those by Maldonado et al[24] indicate that elongation of central photoreceptors in human retina occurs on a more abbreviated timescale than previously reported[1] and may be complete as early as age 18 months. Further exploration of normal ex utero development will facilitate the identification of anatomical aberrations in a clinical setting.

Correspondence: Adam M. Dubis, PhD, Duke University Eye Center, Box 3802 Erwin Rd, Wadsworth Ste 103, Durham, NC 27710 (adam.dubis@gmail.com).

REFERENCES

1. Yuodelis C, Hendrickson A. A qualitative and quantitative analysis of the human fovea during development. *Vision Res.* 1986;26(6):847-855.
2. Hendrickson AE, Yuodelis C. The morphological development of the human fovea. *Ophthalmology.* 1984;91(6):603-612.
3. Diaz-Araya C, Provis JM. Evidence of photoreceptor migration during early foveal development: a quantitative analysis of human fetal retinae. *Vis Neurosci.* 1992;8(6):505-514.
4. Mann I. *The Development of the Human Retina.* New York, NY: Grune & Stratton; 1950.
5. Yamada E. Some structural features of the fovea centralis in the human retina. *Arch Ophthalmol.* 1969;82(2):151-159.
6. Bach L, Seefelder R. *Atlas zur Entwicklungsgeschichte des menschlichen Auges.* Leipzig, Germany: Wilhelm Engelmann; 1914.
7. Abramov I, Gordon J, Hendrickson A, Hainline L, Dobson V, LaBossiere E. The retina of the newborn human infant. *Science.* 1982;217(4556):265-267.
8. Provis JM, Diaz CM, Dreher B. Ontogeny of the primate fovea: a central issue in retinal development. *Prog Neurobiol.* 1998;54(5):549-580.
9. Cornish EE, Madigan MC, Natoli R, Hales A, Hendrickson AE, Provis JM. Gradients of cone differentiation and FGF expression during development of the foveal depression in macaque retina. *Vis Neurosci.* 2005;22(4):447-459.
10. Kozulin P, Natoli R, O'Brien KM, Madigan MC, Provis JM. Differential expression of anti-angiogenic factors and guidance genes in the developing macula. *Mol Vis.* 2009;15:45-59.
11. Kozulin P, Natoli R, Bumsted O'Brien KM, Madigan MC, Provis JM. The cellular expression of antiangiogenic factors in fetal primate macula. *Invest Ophthalmol Vis Sci.* 2010;51(8):4298-4306.
12. Kozulin P, Natoli R, Madigan MC, O'Brien KM, Provis JM. Gradients of *Eph-A6* expression in primate retina suggest roles in both vascular and axon guidance. *Mol Vis.* 2009;15:2649-2662.
13. Springer AD, Troilo D, Possin D, Hendrickson AE. Foveal cone density shows a rapid postnatal maturation in the marmoset monkey. *Vis Neurosci.* 2011;28(6):473-484.
14. Springer AD, Hendrickson AE. Development of the primate area of high acuity, 3: temporal relationships between pit formation, retinal elongation and cone packing. *Vis Neurosci.* 2005;22(2):171-185.
15. Provis JM, Penfold PL, Cornish EE, Sandercoe TM, Madigan MC. Anatomy and development of the macula: specialisation and the vulnerability to macular degeneration. *Clin Exp Optom.* 2005;88(5):269-281.
16. Huang D, Swanson EA, Lin CP, et al. Optical coherence tomography. *Science.* 1991;254(5035):1178-1181.
17. Curcio CA, Messinger JD, Sloan KR, Mitra A, McGwin G, Spaide RF. Human chorioretinal layer thicknesses measured in macula-wide, high-resolution histologic sections. *Invest Ophthalmol Vis Sci.* 2011;52(7):3943-3954.
18. Drexler W, Fujimoto JG. State-of-the-art retinal optical coherence tomography. *Prog Retin Eye Res.* 2008;27(1):45-88.
19. Scott AW, Farsiu S, Enyedi LB, Wallace DK, Toth CA. Imaging the infant retina with a hand-held spectral-domain optical coherence tomography device. *Am J Ophthalmol.* 2009;147(2):364-373.
20. Koozekanani DD, Weinberg DV, Dubis AM, Beringer J, Carroll J. Hemorrhagic retinoschisis in shaken baby syndrome imaged with spectral domain optical coherence tomography. *Ophthalmic Surg Lasers Imaging.* 2010;41:1-3.
21. Chavala SH, Farsiu S, Maldonado R, Wallace DK, Freedman SF, Toth CA. In-

sights into advanced retinopathy of prematurity using handheld spectral domain optical coherence tomography imaging. *Ophthalmology*. 2009;116(12): 2448-2456.

22. Vinekar A, Avadhani K, Sivakumar M, et al. Understanding clinically undetected macular changes in early retinopathy of prematurity on spectral domain optical coherence tomography. *Invest Ophthalmol Vis Sci*. 2011;52(8):5183-5188.

23. Cabrera MT, Maldonado RS, Toth CA, et al. Subfoveal fluid in healthy full-term newborns observed by handheld spectral-domain optical coherence tomography. *Am J Ophthalmol*. 2012;153(1):167-175.

24. Maldonado RS, Izatt JA, Sarin N, et al. Optimizing hand-held spectral domain optical coherence tomography imaging for neonates, infants, and children. *Invest Ophthalmol Vis Sci*. 2010;51(5):2678-2685.

25. Maldonado RS, O'Connell RV, Sarin N, et al. Dynamics of human foveal development after premature birth. *Ophthalmology*. 2011;118(12):2315-2325.

26. Drexler W, Morgner U, Kärtner FX, et al. In vivo ultrahigh-resolution optical coherence tomography. *Opt Lett*. 1999;24(17):1221-1223.

27. Drexler W. Ultrahigh-resolution optical coherence tomography. *J Biomed Opt*. 2004;9(1):47-74.

28. Spaide RF, Curcio CA. Anatomical correlates to the bands seen in the outer retina by optical coherence tomography: literature review and model. *Retina*. 2011; 31(8):1609-1619.

29. Hood DC, Zhang X, Ramachandran R, et al. The inner segment/outer segment border seen on optical coherence tomography is less intense in patients with diminished cone function. *Invest Ophthalmol Vis Sci*. 2011;52(13):9703-9709.

30. Abramoff MD, Magelhaes PJ, Ram SJ. Image processing with ImageJ. *Biophotonics Int*. 2004;11(7):36-42.

31. Vinekar A, Sivakumar M, Shetty R, et al. A novel technique using spectral-domain optical coherence tomography (Spectralis, SD-OCT+HRA) to image supine non-anaesthetized infants: utility demonstrated in aggressive posterior retinopathy of prematurity. *Eye (Lond)*. 2010;24(2):379-382.

32. Wagner-Schuman M, Dubis AM, Nordgren RN, et al. Race- and sex-related differences in retinal thickness and foveal pit morphology. *Invest Ophthalmol Vis Sci*. 2011;52(1):625-634.

33. Dubis AM, Hansen BR, Cooper RF, Beringer J, Dubra A, Carroll J. Relationship between the foveal avascular zone and foveal pit morphology. *Invest Ophthalmol Vis Sci*. 2012;53(3):1628-1636.

Archives Web Quiz Winner

Congratulations to the winner of our May quiz, Anita Agarwal, MD, Vanderbilt Eye Institute, Vanderbilt School of Medicine, Nashville, Tennessee. The correct answer to our May challenge was endogenous endophthalmitis caused by *Salmonella*. For a complete discussion of this case, see the Research Letters section in the June *Archives* (Rachitskaya AV, Flynn HW Jr, Davis JL. Endogenous endophthalmitis caused by *Salmonella* serotype B in an immunocompetent 12-year-old child. *Arch Ophthalmol*. 2012; 130[6]:802-804).
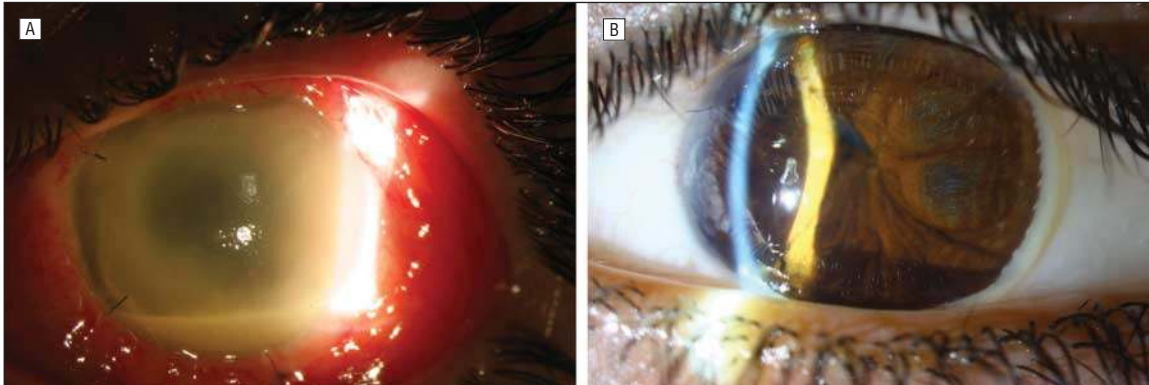
Be sure to visit the *Archives of Ophthalmology* website (http://www.archophthalmol.com) and try your hand at our Clinical Challenge Interactive Quiz. We invite visitors to make a diagnosis based on selected information from a case report or other feature scheduled to be published in the following month's print edition of the *Archives*. The first visitor to e-mail our web editor with the correct answer will be recognized in the print journal and on our website and will receive a 1-year complimentary online subscription to *Archives of Ophthalmology*.